Prepared for submission to JHEP

Neutrino observables from predictive flavour patterns

Luís M. Cebola,[a] **David Emmanuel-Costa,**[a] **and Ricardo González Felipe**[b,a]

[a] *Departamento de Física and Centro de Física Teórica de Partículas - CFTP, Instituto Superior Técnico, Universidade de Lisboa, Avenida Rovisco Pais, 1049-001 Lisboa, Portugal*

[b] *ISEL - Instituto Superior de Engenharia de Lisboa, Instituto Politécnico de Lisboa, Rua Conselheiro Emídio Navarro 1959-007 Lisboa, Portugal*

E-mail: luismcebola@tecnico.ulisboa.pt, david.costa@tecnico.ulisboa.pt, ricardo.felipe@tecnico.ulisboa.pt

Abstract: We look for predictive flavour patterns of the effective Majorana neutrino mass matrix that are compatible with current neutrino oscillation data. Our search is based on the assumption that the neutrino mass matrix contains equal elements and a minimal number of parameters, in the flavour basis where the charged lepton mass matrix is diagonal and real. Three unique patterns that can successfully explain neutrino observables at the 3σ confidence level with just three physical parameters are presented. Neutrino textures described by four and five parameters are also studied. The predictions for the lightest neutrino mass, the effective mass parameter in neutrinoless double beta decays and the CP-violating phases in the leptonic mixing are given.

arXiv:1601.06150v2 [hep-ph] 29 Jan 2016

Contents

1 Introduction 1

2 Minimal neutrino mass matrix textures 2

3 Textures with three parameters 6

4 Textures with four and five parameters 9

5 Conclusions 11

A Summary tables for classes with four and five parameters 12

B Extra correlations among the elements of $\mathbf{m}_\nu$ in class $2_1 1_2 0_2$ 19

References 21

1 Introduction

Neutrino masses constitute a solid evidence of physics beyond the standard model. In the absence of a compelling theory to explain the origin of the lepton flavour structure, one expects the new physics to shed some light in the flavour puzzle. From the theoretical point of view, a natural approach is to restrict the number of free parameters in the lepton flavour sector so that the theory becomes more predictive. One possible framework is to impose the existence of zero elements in the charged lepton and light neutrino mass matrices. Some of such zeroes may simply appear as a result of weak basis transformations [1, 2] while others could be obtained from a symmetry principle [3, 4].

It is well established that neutrino mass matrices with more than two independent zero entries are not compatible with neutrino oscillation data, in the physical basis in which the charged leptons are diagonal and ordered (e,μ,τ). On the other hand, there are several Majorana neutrino patterns with two zeroes that are still viable [5–9]. The latter contain eight real parameters of which five are physical (three unphysical phases can be removed). Another example of predictive textures with five physical parameters are the so-called hybrid textures [10], which have one texture zero and two equal nonzero elements in the physical basis. Most of these hybrid textures are also compatible with current data [9, 11]. Following the same line of reasoning, it is interesting to look for other neutrino textures which have the same predictability or which are even more predictive, i.e., contain less than five physical parameters. Since increasing the number of zeroes is not permitted, a straightforward possibility is to allow for correlations (equalities) of some elements in the effective neutrino mass matrix.

Our knowledge of neutrino masses and leptonic mixing has expanded in the last years thanks to solar, atmospheric, reactor and accelerator neutrino experiments [12–14], as well as to cosmological observations [15]. Leptonic CP violation [16] remains an important open question and it should be probed in near-future neutrino experiments [17]. For light Majorana neutrinos, there are nine specific observables that are relevant in the low-energy neutrino analysis: three neutrino masses, three mixing angles, one Dirac CP phase and two Majorana phases. These parameters should be determined from the physical parameters that characterise a given neutrino mass matrix.

An efficient and reliable approach to confront any neutrino pattern with the observational data is the χ^2-analysis, which we shall use in this work. We shall look for predictive flavour patterns with equal elements (and possibly additional zeroes) in the effective Majorana neutrino mass matrix, and test their compatibility with data at 3σ (99.73%) and 1σ (68.27%) confidence levels (CL).

The paper is organised as follows. In section 2, we describe the minimal neutrino mass matrix textures and present their classification according to the number of physical parameters and correlated matrix elements. The number of solutions compatible with neutrino oscillation data at the 1σ and 3σ CL, for normal (NO) and inverted (IO) mass ordering, are also given. Section 3 is devoted to the search of maximally predictive textures. In particular, it is shown that there exist three unique patterns that can successfully explain neutrino observables at the 3σ CL with just three physical parameters. In section 4, neutrino textures described by four and five physical parameters are discussed. The predictions for the lightest neutrino mass, effective mass parameter in neutrinoless double beta decays and CP-violating phases in the leptonic mixing are also given. Possible breaking paths of the viable three-parameter textures into four- and five-parameter textures compatible with neutrino oscillation data at 1σ are presented. Finally, our concluding remarks are given in section 5.

2 Minimal neutrino mass matrix textures

We shall search for predictive flavour patterns of the effective Majorana neutrino mass matrix $\mathbf{m}_\nu$, based on the assumption that it contains equal matrix elements and, eventually, some vanishing elements. Our analysis is performed in the physical basis where the charged lepton mass matrix is diagonal, real and ordered, i.e., $\mathbf{m}_\ell = \text{diag}\,(m_e, m_\mu, m_\tau)$. Moreover, we restrict our search to neutrino textures with a minimal number of physical parameters, $n < 6$. By physical parameters we mean those that remain after removing all unphysical phases.

In order to classify different textures according to the number of correlated matrix elements, we shall use the notation N_{n_N} to specify that the matrix $\mathbf{m}_\nu$ contains N equal elements and that such correlation appears n_N times in the given texture. In this notation, 1_{n_1} simply denotes n_1 non-vanishing arbitrary elements, while the notation 0_{n_0} will be used to indicate that the neutrino mass matrix has n_0 independent texture zeroes. Since $\mathbf{m}_\nu$ is a 3×3 complex symmetric matrix, it has six independent entries. Clearly, any pattern with more than four equal elements is unrealistic. Thus, in general, we identify any given

n	Texture class	No. of textures	Solutions $(1\sigma, 3\sigma)$		Table in the text
			NO	IO	
2	$4_1 0_2$	7^* ($\subset 15$)	-	-	-
3	$2_2 0_2$	21^* ($\subset 45$)	-	-	-
	$3_1 1_1 0_2$	28^* ($\subset 60$)	-	-	-
	$3_1 2_1 0_1$	60	(0,1)	(0,2)	4
	3_2	10	-	-	-
	$4_1 1_1 0_1$	30	-	-	-
	$4_1 2_1$	15	-	-	-
4	$2_1 1_2 0_2$	42^* ($\subset 90$)	(4,2)	(1,3)	5
	$2_2 1_1 0_1$	90	(15,3)	(19,11)	6, 7
	$3_1 1_2 0_1$	60	(9,3)	(13,10)	8
	$3_1 2_1 1_1$	60	(13,5)	(13,5)	9
	$4_1 1_2$	15	(5,0)	(3,1)	10
5	$1_4 0_2$	7^* ($\subset 15$)	(6,0)	(3,2)	-
	$2_1 1_3 0_1$	60	(31,4)	(36,7)	-
	2_3	15	(4,0)	(1,1)	11
	$3_1 1_3$	20	(19,0)	(18,0)	12

Table 1. Texture classification according to the number of physical parameters n. For each class, the number of different physical textures within the class is given. The number of solutions compatible with data at the 1σ and 3σ CL is also presented. Patterns marked with $*$ are particular cases of the well-known two-zero textures (denoted here as $1_4 0_2$) and, therefore, only the subset of potentially viable matrices are considered. The class $2_1 1_3 0_1$ corresponds to the so-called hybrid textures.

class of textures as $4_{n_4} 3_{n_3} 2_{n_2} 1_{n_1} 0_{n_0}$. The total number of textures for such a class can be determined through the combinatorial relation

$$\frac{6!}{n_4!\,(4!)^{n_4}\,n_3!\,(3!)^{n_3}\,n_2!\,(2!)^{n_2}\,n_1!\,n_0!}\,. \tag{2.1}$$

In table 1 we present the texture classification according to the number of physical parameters n and the correlated matrix elements. For any given texture class, the number of different physical textures within that class is also given. Patterns marked with $*$ are particular cases of the well-known two-zero textures [5] (denoted here as $1_4 0_2$). Only the subset of potentially viable matrices (i.e. patterns $\mathbf{A}_{1,2}$, $\mathbf{B}_{1,2,3,4}$ and $\mathbf{C}$ in the notation of [5]) has been considered [6–9]. Note also that the class $2_1 1_3 0_1$ corresponds to the so-called hybrid textures with two equal elements and one zero [10].

In the next sections we confront all textures in table 1 with the low-energy observational neutrino data. We recall that in the framework of the standard model with three light neutrinos, leptonic mixing is described by the Pontecorvo-Maki-Nakagawa-Sakata unitary matrix $\mathbf{U}$, which relates the mass eigenstate neutrinos ν_i $(i = 1, 2, 3)$ to the flavour eigenstate neutrinos ν_f $(f = e, \mu, \tau)$ [18–20]. This matrix can be parametrised in terms of three mixing angles θ_{12}, θ_{13}, and θ_{23}, a Dirac CP phase δ and two Majorana phases α_{21},

Parameter		Best fit $\pm$ 1σ	3σ
Δm^2_{21} $[10^{-5}\,\mathrm{eV}^2]$		$7.60^{+0.19}_{-0.18}$	7.11 – 8.18
$\lvert\Delta m^2_{31}\rvert$ $[10^{-3}\,\mathrm{eV}^2]$	(NO)	$2.48^{+0.05}_{-0.07}$	2.30 – 2.65
	(IO)	$2.38^{+0.05}_{-0.06}$	2.20 – 2.54
$\sin^2\theta_{12}/10^{-1}$		3.23$\pm$0.16	2.78 – 3.75
$\sin^2\theta_{23}/10^{-1}$	(NO)	$5.67^{+0.32}_{-1.24}$	3.93 – 6.43
	(IO)	$5.73^{+0.25}_{-0.39}$	4.03 – 6.40
$\sin^2\theta_{13}/10^{-2}$	(NO)	2.26$\pm$0.12	1.90 – 2.62
	(IO)	2.29$\pm$0.12	1.93 – 2.65
δ/π	(NO)	$1.41^{+0.55}_{-0.40}$	0.0 – 2.0
	(IO)	1.48$\pm$0.31	0.0 – 2.0

Table 2. Neutrino oscillation parameters at the 68.27% and 99.73% CL [13]. The upper and lower rows in Δm^2_{31}, $\sin^2\theta_{23}$, $\sin^2\theta_{13}$,and δ correspond to NO and IO neutrino masses, respectively.

α_{31} [21]. The neutrino mass matrix $\mathbf{m}_\nu$ is then diagonalised by the unitary transformation

$$\mathbf{U}^\dagger \mathbf{m}_\nu \mathbf{U}^* = \mathrm{diag}\,(m_1, m_2, m_3)\,, \tag{2.2}$$

where m_i are the light neutrino physical masses. The mixing angles are easily reconstructed from $\mathbf{U}$ as

$$\sin^2\theta_{12} = \frac{|U_{12}|^2}{1-|U_{13}|^2}\,, \quad \sin^2\theta_{23} = \frac{|U_{23}|^2}{1-|U_{13}|^2}\,, \quad \sin^2\theta_{13} = |U_{13}|^2\,. \tag{2.3}$$

From the rephasing-invariant quartet $Q \equiv U_{12}U_{23}U^*_{13}U^*_{22}$, the Dirac phase δ can be found through the relations

$$\sin\delta = \frac{8\,\mathrm{Im}\,(Q)}{\cos\theta_{13}\sin 2\theta_{12}\sin 2\theta_{13}\sin 2\theta_{23}}\,, \tag{2.4a}$$

$$\cos\delta = 8\,\frac{\mathrm{Re}\,(Q) + \cos^2\theta_{13}\sin^2\theta_{12}\sin^2\theta_{13}\sin^2\theta_{23}}{\cos\theta_{13}\sin 2\theta_{12}\sin 2\theta_{13}\sin 2\theta_{23}}\,. \tag{2.4b}$$

Finally, the Majorana phases are obtained as

$$\alpha_{21} = 2\arg\left(U^*_{11}U_{12}\right)\,, \quad \alpha_{31} = 2\arg\left(U^*_{11}U_{13}\right) + 2\delta\,. \tag{2.5}$$

Since the absolute scale of neutrino masses is unknown, there are two possible orderings of m_i, namely, a normal ordering (NO) with $m_1 < m_2 < m_3$ or an inverted ordering (IO) with $m_3 < m_1 < m_2$. The mass spectrum may vary from hierarchical to quasi-degenerate, yet cosmological observations place a stringent upper bound on the sum of the masses. Assuming three species of degenerate massive neutrinos and a Λ cold dark matter model, the bound $\sum_i m_i < 0.23$ eV at 95% CL has been obtained from a combined analysis of data [15]. In what follows, we shall assume this bound in our numerical calculations. Notice also that in the physical basis ($\mathbf{m}_\ell$ diagonal) the absolute value of any matrix element of

$\mathbf{m}_\nu$ is always smaller than the largest neutrino mass. Thus the above cosmological bound implies $|m_{\nu ij}| \lesssim 80$ meV.

In our search for viable neutrino mass patterns at 3σ level, we shall consider five observables, namely, the mass-squared differences Δm^2_{21} and Δm^2_{31}, and the mixing angles $\sin^2\theta_{12}$, $\sin^2\theta_{23}$, and $\sin^2\theta_{13}$. When testing the viability of the patterns at 1σ level, the Dirac CP phase δ is also included as an observable quantity. The current neutrino oscillation data are presented in table 2 at the 1σ and 3σ CL [13]. If the predictions for the physical observables are within the ranges given in the table, a texture is considered to be consistent with observations. For such cases, we look for the corresponding predictions for the Dirac CP phase δ, the lightest neutrino mass m, the effective neutrino mass parameter $m_{\beta\beta} = |\sum_i U^2_{ei}\, m_i|$, and the two CP-violating Majorana phases α_{21}, α_{31}. Note that, in the physical basis, one has $m_{\beta\beta} = |m_{\nu ee}| \lesssim 80$ meV, for all textures considered in this work.

Concerning the atmospheric mixing angle θ_{23}, it is worth noticing that its value is close to maximal ($\theta_{23} \approx \pi/4$). Starting from a given texture $\mathbf{m}_\nu$, one can always define a new texture $\mathbf{m}'_\nu$, whose observables are directly related to those of $\mathbf{m}_\nu$,

$$\mathbf{m}'_\nu = \mathbf{P}_{23}\, \mathbf{m}_\nu\, \mathbf{P}_{23}\,. \tag{2.6}$$

Here $\mathbf{P}_{23}$ is the permutation matrix acting in the sector $(2,3)$. Said otherwise, $\mathbf{m}'_\nu$ is obtained from $\mathbf{m}_\nu$ by interchanging its second and third rows and columns. The matrices $\mathbf{m}_\nu$ and $\mathbf{m}'_\nu$ share the same mass spectrum, mixing angles θ_{12} and θ_{13}, and Majorana phases α_{21}, α_{31}, while the mixing angle θ_{23} and the Dirac phase δ are transformed as

$$\theta_{23} \;\to\; \frac{\pi}{2} - \theta_{23}\,, \quad \delta \;\to\; \delta - \pi\,. \tag{2.7}$$

One can then conclude from table 2 that, if the given texture $\mathbf{m}_\nu$ is viable at 3σ CL, the transformed $\mathbf{m}'_\nu$ would also be compatible with neutrino oscillation data, provided that $\sin^2\theta_{23} \leq 0.6$ (i.e. $\theta_{23} \leq 51^\circ$) in both NO and IO cases.

We shall perform a χ^2-analysis using the standard definition of the χ^2-function in terms of the observable values and their deviations from the mean values. The minimisation of the χ^2 function is carried out with respect to the neutrino observables using the MINUIT package [22], following the numerical strategy presented in [9]. This procedure allows us to determine whether a given pattern is compatible at 1σ level. In order to obtain the allowed ranges at 3σ CL for the predictable quantities, we then randomly scan the full parameter space in the neutrino mass matrices. Since we do not impose any restriction on the complex matrix elements $m_{\nu ij}$, our solutions exhibit an explicit symmetry on the CP phases:

$$\delta \to -\delta\,, \quad \alpha_{21} \to -\alpha_{21}\,, \quad \alpha_{31} \to -\alpha_{31}\,. \tag{2.8}$$

Since this symmetry does not change the value of any other observable or prediction, we use it to restrict the Dirac phase to the range $0 \leq \delta \leq \pi$ when presenting our results. Obviously, values of δ in the range $\pi \leq \delta \leq 2\pi$ are physical as well and may be even preferred by the experimental data [23] (cf. also table 2).

In the next sections, we seek for minimal neutrino textures that fulfil our criteria, i.e., that contain equal or vanishing elements and simultaneously have a minimal number of

physical parameters. Since $\mathbf{m}_\nu$ is symmetric, we shall use the following sequential notation to label the position of the matrix elements of a given neutrino texture T,

$$\begin{pmatrix} 1 & 2 & 3 \\ 2 & 4 & 5 \\ 3 & 5 & 6 \end{pmatrix} . \tag{2.9}$$

We denote the position of any vanishing element labeled i with a superscript, i.e. T^i, while equal elements with labels $i, j, \ldots, k$ are listed as subscripts, $\mathsf{T}_{ij\ldots k}$. For instance, the notations $\mathsf{T}^{5,6}_{12,34}$ and $\mathsf{T}^{6}_{123,45}$ correspond to the textures

$$\mathsf{T}^{5,6}_{12,34} = \begin{pmatrix} a & a & b \\ a & b & 0 \\ b & 0 & 0 \end{pmatrix} \quad \text{and} \quad \mathsf{T}^{6}_{123,45} = \begin{pmatrix} a & a & a \\ a & b & b \\ a & b & 0 \end{pmatrix} , \tag{2.10}$$

respectively.

3 Textures with three parameters

Following our χ^2 numerical strategy, we have analysed all possible textures belonging to the classes listed in table 1. The number of solutions compatible with neutrino oscillation data at the 1σ and 3σ CL are reported in this table.[1] From our search of the different pattern classes, no solution with only two physical parameters (class $4_1 0_2$) was found, neither for NO nor for IO neutrino spectrum. Thus, we conclude that under our assumptions (equal or vanishing elements) the minimal number of free physical parameters is 3. Moreover, from the table, one can see that the only viable class with $n = 3$ is $3_1 2_1 0_1$. Out of the 60 textures within this class, only the patterns $\mathsf{T}^{2}_{136,45}$ for NO neutrino spectrum and $\mathsf{T}^{4}_{123,56}$ and $\mathsf{T}^{6}_{123,45}$ for IO spectrum are compatible with data at the 3σ level. None of the textures passed the 1σ CL test.

For the texture $\mathsf{T}^{2}_{136,45}$ the effective neutrino mass matrix $\mathbf{m}_\nu$ has the following form

$$\mathbf{m}_\nu \equiv \begin{pmatrix} a & 0 & a \\ 0 & b & b \\ a & b & a \end{pmatrix} . \tag{3.1}$$

The minimum of χ^2 for this solution is $\chi^2_{\rm min} = 6.68$. An example that leads to this value is given by the choice of $a = 10.5731$ meV and $|b| = 29$ meV, $\arg b = 0.08284\pi$. This in turn yields the following low-energy neutrino parameters:

$$\begin{aligned} &\Delta m^2_{21} = 7.61 \times 10^{-5}\,\text{eV}^2, \quad |\Delta m^2_{31}| = 2.47 \times 10^{-3}\,\text{eV}^2, \\ &\sin^2\theta_{12} = 3.14 \times 10^{-1}, \quad \sin^2\theta_{23} = 6.31 \times 10^{-1}, \quad \sin^2\theta_{13} = 2.44 \times 10^{-2} . \end{aligned} \tag{3.2}$$

[1] Note that the number of solutions at 3σ refers to the number of textures that are consistent with data at 3σ but not at 1σ CL.

It also predicts

$$\begin{aligned} m_1 = 12\,\text{meV}, \quad m_2 = 15\,\text{meV}, \quad m_3 = 51\,\text{meV}, \quad m_{\beta\beta} = 11\,\text{meV}, \\ \delta = 0.41\pi, \quad \alpha_{21} = 1.5\pi, \quad \alpha_{31} = 0.70\pi\,. \end{aligned} \tag{3.3}$$

Similarly, for the texture $\mathsf{T}^4_{123,56}$ corresponding to

$$\mathbf{m}_\nu \equiv \begin{pmatrix} a & a & a \\ a & 0 & b \\ a & b & b \end{pmatrix}\,, \tag{3.4}$$

the minimum of χ^2 is given by $\chi^2_{\rm min} = 5.96$. This minimum is obtained if we take, for instance, $a = 28.56$ meV and $|b| = 18.8744$ meV, $\arg b = 1.00845\pi$, which lead to the low-energy neutrino parameters

$$\begin{aligned} \Delta m^2_{21} = 7.59 \times 10^{-5}\,\text{eV}^2, \quad |\Delta m^2_{31}| = 2.38 \times 10^{-3}\,\text{eV}^2, \\ \sin^2\theta_{12} = 3.25 \times 10^{-1}, \quad \sin^2\theta_{23} = 5.74 \times 10^{-1}, \quad \sin^2\theta_{13} = 2.57 \times 10^{-2}\,, \end{aligned} \tag{3.5}$$

and the predictions

$$\begin{aligned} m_1 = 50\,\text{meV}, \quad m_2 = 51\,\text{meV}, \quad m_3 = 10\,\text{meV}, \quad m_{\beta\beta} = 29\,\text{meV}, \\ \delta = 0.32\pi, \quad \alpha_{21} = 1.3\pi, \quad \alpha_{31} = 0.49\pi. \end{aligned} \tag{3.6}$$

Finally, for the texture $\mathsf{T}^6_{123,45}$ one has

$$\mathbf{m}_\nu \equiv \begin{pmatrix} a & a & a \\ a & b & b \\ a & b & 0 \end{pmatrix}\,. \tag{3.7}$$

In this case, the minimum of χ^2 corresponds to a somewhat larger value, $\chi^2_{\rm min} = 20.00$, which can be reached, e.g., with $a = 28.56$ meV and $|b| = 18.8746$ meV, $\arg b = 0.99155\pi$, leading to the following low-energy neutrino observables:

$$\begin{aligned} \Delta m^2_{21} = 7.59 \times 10^{-5}\,\text{eV}^2, \quad |\Delta m^2_{31}| = 2.38 \times 10^{-3}\,\text{eV}^2, \\ \sin^2\theta_{12} = 3.25 \times 10^{-1}, \quad \sin^2\theta_{23} = 4.26 \times 10^{-1}, \quad \sin^2\theta_{13} = 2.57 \times 10^{-2}\,. \end{aligned} \tag{3.8}$$

The predicted mass spectrum and CP-violating phases are

$$\begin{aligned} m_1 = 50\,\text{meV}, \quad m_2 = 51\,\text{meV}, \quad m_3 = 10\,\text{meV}, \quad m_{\beta\beta} = 29\,\text{meV}, \\ \delta = 0.68\pi, \quad \alpha_{21} = 0.67\pi, \quad \alpha_{31} = 1.5\pi. \end{aligned} \tag{3.9}$$

For each texture, we have also performed a random scan of the input parameters a and b in order to determine the viable ranges at 3σ for the quantities δ, m, $m_{\beta\beta}$, α_{21} and α_{31}. The results are collected in table 4 of appendix A for the textures $\mathsf{T}^2_{136,45}$, $\mathsf{T}^4_{123,56}$ and $\mathsf{T}^6_{123,45}$. From the table one sees that neutrino observables are quite constrained in the three cases. In particular, for the texture $\mathsf{T}^2_{136,45}$ the Majorana phase α_{21} is predicted to be approximatively $3\pi/2$.

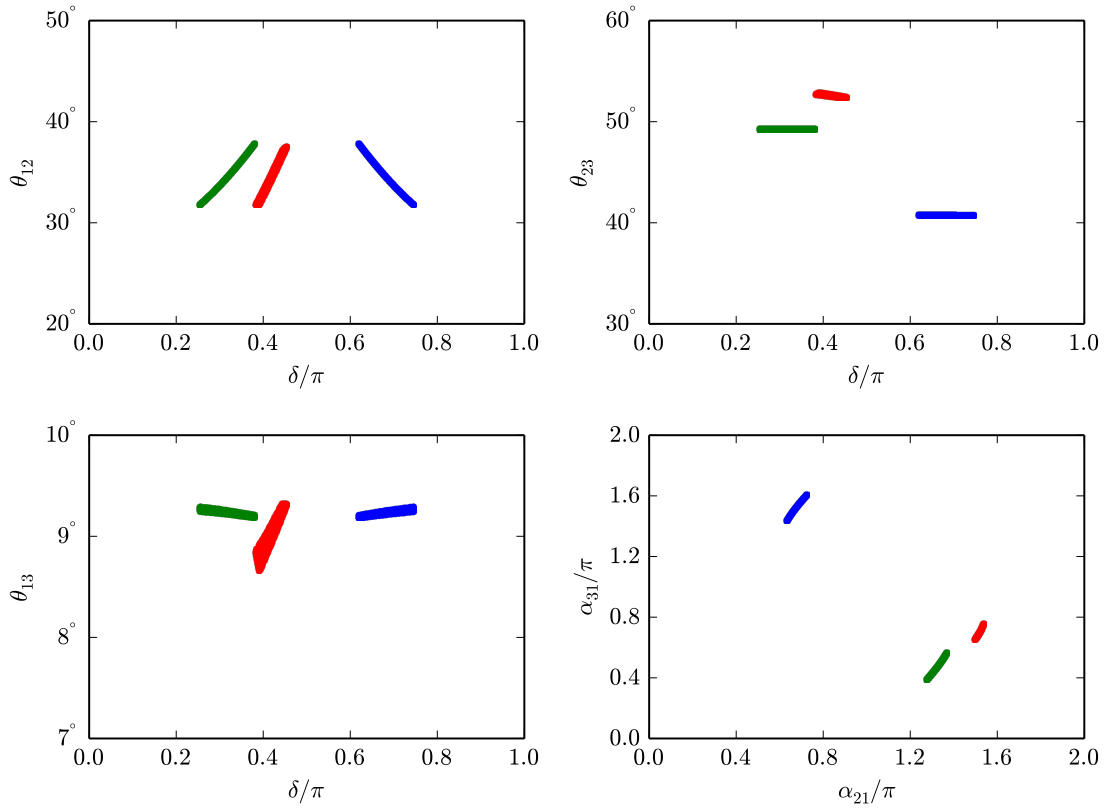

Figure 1. Predictions for 3-parameter textures $\mathsf{T}^2_{136,45}$ (NO, red points), $\mathsf{T}^4_{123,56}$ (IO, green points) and $\mathsf{T}^6_{123,45}$ (IO, blue points).

In figure 1, we show the correlation of the Dirac phase δ with the three mixing angles, as well as the correlation between the Majorana phases. Notice that in virtue to the symmetry (2.8) we restrict the values of δ to $[0, \pi]$. The effective mass parameter $m_{\beta\beta}$ as a function of the lightest neutrino mass m is plotted in figure 2(a). As can be seen in the figure, the predicted values for $m_{\beta\beta}$ are not far away from the values expected in the future CUORE [24] and SuperNEMO [25] $0\nu\beta\beta$ experiments.

Notice that the textures $\mathsf{T}^4_{123,56}$ and $\mathsf{T}^6_{123,45}$ are related through the transformation given in equation (2.6) and, therefore, their predictions are similar, except for the mixing angle θ_{23} and the Dirac phase δ that are transformed according to equation (2.7). We remark that for the Majorana phases α_{21} and α_{31} this conclusion may not be obvious in table 4 and the numerical examples presented above, since after bringing the value of δ to the range $[0, \pi]$, the Majorana phases flip their signs. For the case of the texture $\mathsf{T}^2_{136,45}$, one has necessarily $\sin^2\theta_{23} > 0.6$, i.e., $\theta_{23} > 51^\circ$ (see figure 1) and thus the transformed texture obtained from equation (2.6) does not lead to a viable neutrino pattern.

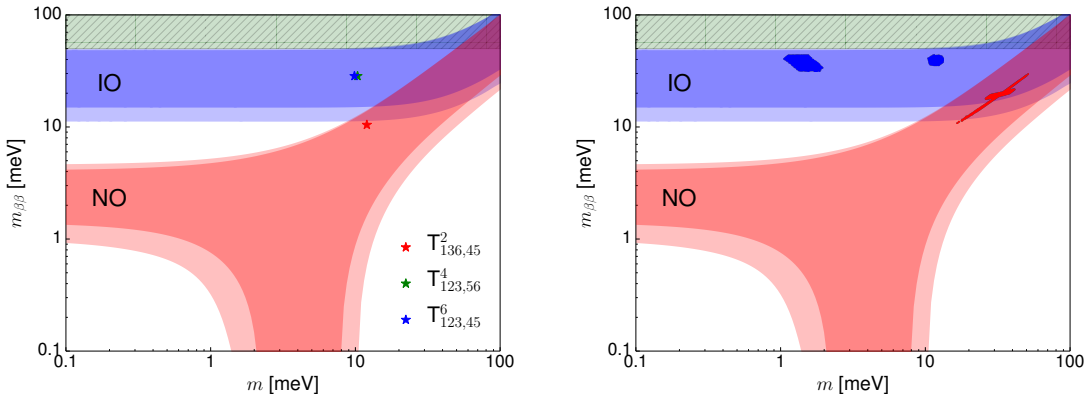

(a) Class $3_1 2_1 0_1$ (b) Class $4_1 1_2$

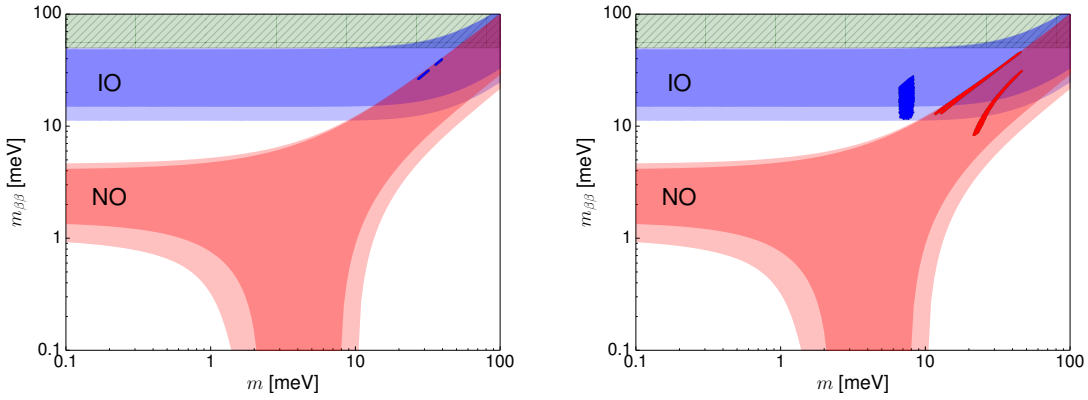

(c) Class $2_1 1_2 0_2$ (d) Class 2_3

Figure 2. Predictions for $m_{\beta\beta}$ for different texture classes with NO (red colour) and IO (blue colour). The inner dark bands correspond to the 1σ neutrino oscillation parameters, while the lighter outer bands include the 3σ uncertainties. The green horizontal band corresponds to the expected sensitivity in near future of $0\nu\beta\beta$ experiments.

4 Textures with four and five parameters

In this section, we consider the remaining classes in table 1 and look for solutions with four and five physical parameters compatible with low-energy neutrino data at 3σ CL, and eventually consistent with data at 1σ. As it turns out, all classes (with $n = 4, 5$) contain viable solutions at 1σ CL. In appendix A, the predictions of the corresponding neutrino textures are summarised in tables 5–10 for $n = 4$ and tables 11 and 12 for $n = 5$. As before, the values of δ are restricted to $[0, \pi]$. We remark that the five-parameter textures belonging to the classes $1_4 0_2$ and $2_1 1_3 0_1$ are not considered, since they have been studied in [9].

From the tables, we conclude that textures within the same class do not share necessarily the same predictions. Remarkably, some of the classes predict a quite constrained

region in the plane $(m, m_{\beta\beta})$, namely the classes $4_1 1_2$, $2_1 1_2 0_2$ and 2_3, as shown in figures 3, 2(c) and 2(d), respectively. It can also be noticed from the tables that there exist two disconnected δ-regions for certain textures and, in some cases, the value of the Majorana phase α_{21} is essentially fixed.

It is interesting to note that the class $2_1 1_2 0_2$, which is more restrictive than the two-zero textures in $1_4 0_2$, is also compatible with the data at both 1σ and 3σ CL. More precisely, three textures of the class $1_4 0_2$, compatible with data at 1σ, give rise to viable patterns in class $2_1 1_2 0_2$. The textures A_1 and A_2 lead, for NO, to the textures $A_{1,45}$, $A_{1,46}$, $A_{2,46}$, $A_{2,56}$ (compatible at 1σ CL), and the textures $A_{1,56}$, $A_{2,45}$ (compatible only at 3σ CL). The remaining texture C of class $1_4 0_2$ leads, for IO, to four textures within class $2_1 1_2 0_2$: C_{13} (compatible at 1σ CL) and C_{12}, C_{25}, C_{35} (compatible only at 3σ CL). In labelling the above textures, we have used the notation of [5] for the $1_4 0_2$ textures and denoted the pair of equal elements in the corresponding textures of class $2_1 1_2 0_2$ with an extra subscript pair. Note also that the class $2_1 1_2 0_2$ is the only viable class with textures having an additional correlation among the matrix elements of the two-zero textures of class $1_4 0_2$. Particular cases of textures belonging to the class $2_1 1_2 0_2$ have been previously considered in the literature. For example, the texture C_{25} was analysed in [26], while the textures $A_{1,46}$ and $A_{2,46}$ with an additional constraint were found to be compatible with data at 3σ CL in [27]. We analysed all the textures of table 5 in order to search for extra correlations among the matrix elements of $\mathbf{m}_\nu$. Besides the two textures given in [27], we have found eight new textures that are consistent with observations at 3σ CL. Remarkably, there are also four patterns with only three physical parameters that can accommodate the neutrino data at 1σ CL. A summary of these results is presented in appendix B.

In section 3, we have shown that the three-parameter textures $\mathsf{T}^2_{136,45}$ (for NO neutrino spectrum), $\mathsf{T}^4_{123,56}$ and $\mathsf{T}^6_{123,45}$ (for IO spectrum) are compatible with data at the 3σ CL. Assuming that these patterns could be implemented through symmetries, one may wonder whether they can be made compatible with neutrino oscillation data at the 1σ CL, once the symmetries are (softly) broken. Since the above patterns belong to the texture class $3_1 2_1 0_1$, four natural breaking paths can be envisaged: the breaking to the classes $3_1 2_1 1_1$, $3_1 1_2 0_1$, $2_2 1_1 0_1$ or $2_1 1_3 0_1$, obtained from the initial class $3_1 2_1 0_1$ by breaking the zero entry, the doublet or the triplet (one or two elements), respectively. Let us analyse each possibility in detail.

Looking at tables 8 and 9 we can easily verify that the breaking paths $\mathsf{T}^2_{136,45} \to \mathsf{T}_{136,45}$ and $\mathsf{T}^2_{136,45} \to \mathsf{T}^2_{136}$ are not viable either for NO or IO mass spectrum. From table 6 we also conclude that the pattern $\mathsf{T}^2_{36,45}$ is not compatible with data at 1σ. On the other hand, the textures $\mathsf{T}^2_{13,45}$ and $\mathsf{T}^2_{16,45}$ turn out to be viable for NO spectrum. Finally, the breaking $\mathsf{T}^2_{136,45} \to \mathsf{T}^2_{45}$ results in a hybrid texture that is compatible with data for both NO and IO neutrino mass spectra [9]. We note that in the notation of [9] the texture T^2_{45} corresponds to the matrix $\widehat{\mathbf{D}}_{1(12)}$.

Let us now consider the texture $\mathsf{T}^4_{123,56}$. In this case, breaking it to the classes $3_1 2_1 1_1$ and $3_1 1_2 0_1$ yields the viable patterns $\mathsf{T}_{123,56}$ and T^4_{123} for IO spectrum, as can be seen from tables 8 and 9. Similarly, the breaking path to the class $2_2 1_1 0_1$, which contains two pairs of equal elements, leads to three textures compatible with data, $\mathsf{T}^4_{12,56}$, $\mathsf{T}^4_{13,56}$, and $\mathsf{T}^4_{23,56}$,

Texture	$3_1 2_1 1_1$	$3_1 1_2 0_1$	$2_2 1_1 0_1$	$2_1 1_3 0_1$
$\mathsf{T}^2_{136,45}$	$\mathsf{T}_{136,45}$ (-)	T^2_{136} (-)	$\mathsf{T}^2_{13,45}$ (NO) $\mathsf{T}^2_{16,45}$ (NO) $\mathsf{T}^2_{36,45}$ (-)	T^2_{45} (NO, IO)
$\mathsf{T}^4_{123,56}$	$\mathsf{T}_{123,56}$ (IO)	T^4_{123} (IO)	$\mathsf{T}^4_{12,56}$ (IO) $\mathsf{T}^4_{13,56}$ (IO) $\mathsf{T}^4_{23,56}$ (IO)	T^4_{56} (IO)
$\mathsf{T}^6_{123,45}$	$\mathsf{T}_{123,45}$ (IO)	T^6_{123} (-)	$\mathsf{T}^6_{12,45}$ (-) $\mathsf{T}^6_{13,45}$ (-) $\mathsf{T}^6_{23,45}$ (-)	T^6_{45} (IO)

Table 3. Neutrino mass textures arising from the breaking of either the texture zero or the equality of elements in the three-parameter matrices of table 4. Their compatibility with data at 1σ is also shown.

all of them for an IO neutrino spectrum (cf. table 7). Furthermore, there is also a viable pattern within the hybrid class $2_1 1_3 0_1$, namely, the matrix T^4_{56} (or $\widehat{\mathbf{D}}_{2(22)}$ in the notation of [9]).

Finally, for the texture $\mathsf{T}^6_{123,45}$, only the paths $\mathsf{T}^6_{123,45} \to \mathsf{T}_{123,45}$ and $\mathsf{T}^6_{123,45} \to \mathsf{T}^6_{45}$ (or $\widehat{\mathbf{D}}_{1(33)}$ in the notation of [9]) turn out to be viable, both of them for an IO neutrino mass spectrum. A summary of the breaking paths for the three-parameter textures is presented in table 3.

5 Conclusions

Despite the overwhelming success of the standard model, the nature of the flavour structure of the quark and lepton sectors is still unknown. One of the common approaches to address this puzzle is to assume certain constraints on the mass matrices in order to reduce the number of free parameters.

In this paper, we looked for predictive flavour patterns of the effective Majorana neutrino mass matrix that are compatible with current neutrino oscillation data at the 3σ CL. Our study was based on the assumption that the effective neutrino mass matrix contains some restrictions in the physical basis where the charged leptons are diagonal and properly ordered. In particular, we assumed the existence of equal matrix elements or the presence of texture zeroes (see table 1). Following a standard χ^2-analysis, we found three unique patterns that are described by just three physical parameters and can successfully explain current neutrino data at the 3σ CL. The predictions of these solutions for the neutrino observables, namely, the lightest neutrino mass, the effective mass parameter in neutrinoless double beta decays, and the CP-violating phases, are summarised in table 4.

We have also studied neutrino textures described by four and five physical parameters. Several viable patterns were found to be compatible with the data at 1σ and 3σ CL. Their predictions are given in tables 5–10 for $n = 4$ and tables 11 and 12 for $n = 5$. From our study we can conclude that current neutrino data do not allow to discriminate, among the viable

predictive neutrino mass matrix textures, the patterns that more appropriately describe the observations. Upcoming neutrino experiments and more precise future measurements could shed some light on this issue.

The neutrino textures considered in this work were taken as simple and economical anzätze. It would be interesting to see if such predictive textures could arise from a symmetry principle. For instance, it has been shown that the two-zero textures in class $1_4 0_2$ can be obtained from continuous or discrete flavour symmetries (see e.g. [4, 6, 28]), while the particular texture $\mathsf{T}^{4,6}_{25}$ of class $2_1 1_2 0_2$ can be constructed through a flavour symmetry based on the order-twelve quaternion group Q_6 [26]. Similarly, the hybrid textures belonging to class $2_1 1_3 0_1$ can be realised in a type-II seesaw framework by implementing certain discrete symmetries [11]. Another aspect that deserves further study is the stability of the textures under the renormalisation group evolution.

Acknowledgments

The authors acknowledge support from Fundação para a Ciência e a Tecnologia (FCT, Portugal) through the projects CERN/FIS-NUC/0010/2015 and UID/FIS/00777/2013. L.C. is supported by FCT under the contract PD/BD/113479/2015.

A Summary tables for classes with four and five parameters

In this appendix we summarise the predictions for the Dirac CP phase δ, the lightest neutrino mass m, the effective neutrino mass parameter $m_{\beta\beta}$, and the two CP-violating Majorana phases α_{21}, α_{31} for all the viable textures listed in table 1. The results for $n = 3$, $n = 4$, and $n = 5$ physical parameters are given in table 4, tables 5–10, and tables 11, 12, respectively.

Spectrum	Texture	δ/π	m [meV]	$m_{\beta\beta}$ [meV]	α_{21}/π	α_{31}/π	1σ CL
NO	$\mathsf{T}^2_{136,45}$	0.38 – 0.45	11 – 13	9.9 – 11	≈ 1.5	0.66 – 0.75	-
IO	$\mathsf{T}^4_{123,56}$	0.26 – 0.38	9.7 – 11	27 – 30	1.3 – 1.4	0.39 – 0.56	-
	$\mathsf{T}^6_{123,45}$	0.62 – 0.74	9.7 – 10	27 – 30	0.63 – 0.72	1.4 – 1.6	-

Table 4. Neutrino mass textures in class $3_1 2_1 0_1$ compatible with data at 3σ CL.

Spectrum	Texture	δ/π	m [meV]	$m_{\beta\beta}$ [meV]	α_{21}/π	α_{31}/π	1σ CL
NO	$\mathsf{T}^{1,3}_{45}$	0.0 – 1.0	2.6 – 8.9	0	1.0 – 1.1	1.0 – 2.0	-
	$\mathsf{T}^{1,2}_{45}$	0.26 – 0.62	4.1 – 5.9	0	0.88 – 0.93	0.22 – 0.54	✓
	$\mathsf{T}^{1,3}_{46}$	0.0 – 1.0	3.9 – 6.7	0	1.0 – 1.1	1.0 – 2.0	✓
	$\mathsf{T}^{1,2}_{46}$	0.0 – 1.0	3.9 – 6.6	0	0.89 – 1.0	0.0 – 1.0	✓
	$\mathsf{T}^{1,3}_{56}$	0.31 – 0.75	4.1 – 5.9	0	≈ 1.1	1.4 – 1.8	✓
	$\mathsf{T}^{1,2}_{56}$	0.0 – 1.0	2.7 – 8.9	0	0.89 – 1.0	0.0 – 1.0	-
IO	$\mathsf{T}^{4,6}_{12}$	0.27 – 0.38	36 – 39	36 – 39	1.3 – 1.4	0.43 – 0.58	-
		0.63 – 0.80	29 – 32	29 – 32	0.68 – 0.80	1.5 – 1.7	
	$\mathsf{T}^{4,6}_{13}$	0.61 – 0.73	36 – 39	36 – 39	0.61 – 0.69	1.4 – 1.6	✓
	$\mathsf{T}^{4,6}_{25}$	0.27 – 0.38	35 – 38	35 – 38	1.3 – 1.4	0.41 – 0.57	-
		0.65 – 0.84	27 – 31	27 – 30	0.69 – 0.84	1.5 – 1.8	
	$\mathsf{T}^{4,6}_{35}$	0.62 – 0.73	35 – 38	35 – 38	0.62 – 0.71	1.4 – 1.6	-

Table 5. Neutrino mass textures in class $2_1 1_2 0_2$ compatible with data at 3σ CL.

Spectrum	Texture	δ/π	m [meV]	$m_{\beta\beta}$ [meV]	α_{21}/π	α_{31}/π	1σ CL
NO	$\mathsf{T}^{3}_{12,45}$	0.063 – 1.0	6.2 – 15	7.4 – 13	0.33 – 1.6	0.10 – 1.7	✓
	$\mathsf{T}^{3}_{12,46}$	0.0 – 1.0	7.3 – 19	8.0 – 15	0.38 – 1.6	0.0 – 2.0	✓
	$\mathsf{T}^{3}_{12,56}$	0.072 – 0.47	7.2 – 11	8.1 – 10	0.35 – 0.48	0.61 – 1.2	✓
		0.79 – 1.0	11 – 14	9.6 – 12	0.41 – 1.7	0.12 – 1.7	
	$\mathsf{T}^{2}_{13,45}$	0.0 – 0.82	8.4 – 13	8.5 – 12	0.39 – 1.6	0.25 – 1.8	✓
	$\mathsf{T}^{2}_{13,46}$	0.0 – 1.0	7.3 – 19	8.0 – 15	0.36 – 1.6	0.0 – 2.0	✓
	$\mathsf{T}^{2}_{13,56}$	0.0 – 0.20	9.0 – 17	8.8 – 14	0.36 – 1.6	0.31 – 2.0	✓
		0.55 – 0.96	6.4 – 15	7.5 – 13	1.5 – 1.6	0.98 – 1.3	
	$\mathsf{T}^{3}_{14,26}$	0.48 – 0.61	22 – 26	23 – 27	0.081 – 0.12	0.98 – 1.2	-
	$\mathsf{T}^{2}_{14,36}$	0.36 – 0.56	22 – 29	22 – 29	1.8 – 1.9	0.75 – 1.0	✓
	$\mathsf{T}^{3}_{14,56}$	0.19 – 0.33	16 – 44	16 – 45	0.051 – 0.31	0.52 – 0.89	✓
		0.83 – 0.89	17 – 44	17 – 45	0.056 – 0.32	1.5 – 1.6	
	$\mathsf{T}^{2}_{14,56}$	0.12 – 0.17	22 – 47	22 – 47	1.8 – 1.9	0.41 – 0.49	✓
		0.75 – 0.81	21 – 49	22 – 49	≈ 1.9	1.3 – 1.5	
	$\mathsf{T}^{3}_{15,46}$	0.0 – 1.0	19 – 70	16 – 70	0.024 – 1.8	0.0 – 2.0	✓
	$\mathsf{T}^{2}_{15,46}$	0.0 – 1.0	19 – 71	16 – 71	0.16 – 2.0	0.0 – 2.0	✓
	$\mathsf{T}^{3}_{16,24}$	0.47 – 0.62	21 – 25	22 – 26	0.14 – 0.19	1.0 – 1.2	-
	$\mathsf{T}^{3}_{16,45}$	0.19 – 0.34	14 – 42	15 – 42	0.076 – 0.19	0.53 – 0.82	✓
		0.82 – 0.88	15 – 45	16 – 45	0.088 – 0.21	1.4 – 1.6	
	$\mathsf{T}^{2}_{16,45}$	0.11 – 0.81	11 – 41	9.7 – 42	1.5 – 1.9	0.41 – 1.5	✓
	$\mathsf{T}^{3}_{25,46}$	0.076 – 0.87	22 – 70	18 – 68	1.7 – 1.9	0.0 – 2.0	✓
	$\mathsf{T}^{2}_{35,46}$	0.13 – 0.92	22 – 71	18 – 70	0.095 – 0.34	0.0 – 2.0	✓
	$\mathsf{T}^{2}_{36,45}$	0.22 – 0.53	11 – 15	9.2 – 14	1.4 – 1.6	0.45 – 0.88	-

Table 6. Neutrino mass textures in class $2_2 1_1 0_1$ compatible with data at 3σ CL for NO spectrum.

Spectrum	Texture	δ/π	m [meV]	$m_{\beta\beta}$ [meV]	α_{21}/π	α_{31}/π	1σ CL
IO	$\mathsf{T}^5_{12,34}$	0.0 – 1.0	30 – 39	29 – 39	0.63 – 1.4	0.43 – 1.6	✓
	$\mathsf{T}^5_{12,36}$	0.0 – 0.34	30 – 36	31 – 36	0.63 – 1.3	0.43 – 1.6	✓
		0.57 – 0.99	30 – 36	31 – 36	1.2 – 1.4	1.3 – 1.6	
	$\mathsf{T}^6_{12,45}$	0.44 – 0.91	9.7 – 14	27 – 30	0.62 – 0.72	1.3 – 1.7	-
	$\mathsf{T}^5_{12,46}$	0.12 – 0.29	29 – 38	28 – 38	0.62 – 0.81	0.44 – 0.67	✓
		0.67 – 0.89	29 – 37	28 – 37	1.2 – 1.4	1.2 – 1.6	
	$\mathsf{T}^4_{12,56}$	0.0 – 0.71	9.8 – 17	26 – 30	0.67 – 1.4	0.16 – 1.5	✓
	$\mathsf{T}^5_{13,24}$	0.0 – 0.35	32 – 36	32 – 36	0.63 – 1.4	0.42 – 1.6	✓
		0.60 – 0.97	32 – 36	32 – 37	1.3 – 1.4	1.4 – 1.6	
	$\mathsf{T}^5_{13,26}$	0.0 – 1.0	30 – 38	29 – 38	0.61 – 1.4	0.41 – 1.6	✓
	$\mathsf{T}^6_{13,45}$	0.42 – 0.94	9.8 – 14	27 – 30	0.63 – 0.74	1.3 – 1.8	-
	$\mathsf{T}^5_{13,46}$	0.095 – 0.27	31 – 40	30 – 40	0.60 – 0.75	0.38 – 0.66	✓
		0.73 – 0.88	30 – 41	30 – 40	1.2 – 1.4	1.4 – 1.6	
	$\mathsf{T}^4_{13,56}$	0.0 – 0.68	9.7 – 17	27 – 32	0.66 – 1.4	0.24 – 1.4	✓
	$\mathsf{T}^6_{14,23}$	0.22 – 1.0	0.53 – 27	13 – 17	0.83 – 1.1	0.0 – 2.0	-
	$\mathsf{T}^5_{14,23}$	0.042 – 0.90	12 – 65	12 – 65	0.45 – 1.6	0.29 – 1.7	✓
	$\mathsf{T}^6_{14,25}$	0.0 – 0.90	49 – 65	27 – 32	0.77 – 1.2	0.0049 – 2.0	✓
	$\mathsf{T}^5_{14,26}$	0.077 – 0.24	27 – 38	27 – 37	0.63 – 0.83	0.45 – 0.69	✓
		0.60 – 0.84	27 – 37	27 – 36	1.2 – 1.4	1.2 – 1.6	
	$\mathsf{T}^5_{14,36}$	0.068 – 0.32	26 – 37	24 – 37	0.63 – 0.90	0.40 – 0.88	✓
		0.48 – 0.83	26 – 37	24 – 37	1.1 – 1.4	1.1 – 1.5	
	$\mathsf{T}^6_{15,23}$	0.0 – 0.87	14 – 66	12 – 66	0.44 – 1.6	0.0 – 2.0	-
	$\mathsf{T}^4_{15,23}$	0.13 – 1.0	15 – 65	12 – 65	0.41 – 1.6	0.0 – 2.0	✓
	$\mathsf{T}^5_{16,23}$	0.097 – 0.95	13 – 66	12 – 65	0.44 – 1.6	0.29 – 1.7	-
	$\mathsf{T}^4_{16,23}$	0.0 – 0.83	0.53 – 27	13 – 17	0.85 – 1.2	0.0 – 2.0	✓
	$\mathsf{T}^5_{16,24}$	0.18 – 0.93	24 – 36	21 – 36	0.64 – 1.4	0.47 – 1.6	✓
	$\mathsf{T}^5_{16,34}$	0.15 – 0.35	29 – 40	29 – 39	0.62 – 0.78	0.39 – 0.69	✓
		0.77 – 0.93	29 – 40	29 – 39	1.2 – 1.4	1.3 – 1.5	
	$\mathsf{T}^4_{16,35}$	0.25 – 0.99	54 – 65	29 – 32	0.79 – 1.2	0.012 – 2.0	-
	$\mathsf{T}^6_{23,45}$	0.62 – 0.90	7.7 – 11	22 – 30	0.62 – 0.91	1.4 – 1.9	-
	$\mathsf{T}^4_{23,56}$	0.095 – 0.39	7.7 – 11	22 – 30	1.1 – 1.4	0.14 – 0.58	✓
	$\mathsf{T}^5_{24,36}$	0.0 – 0.33	31 – 35	32 – 35	0.65 – 0.75	0.42 – 0.65	✓
		0.62 – 0.96	32 – 35	32 – 35	1.2 – 1.4	1.3 – 1.6	
	$\mathsf{T}^4_{25,36}$	0.35 – 0.42	12 – 14	36 – 38	≈ 1.5	0.58 – 0.68	-
	$\mathsf{T}^3_{25,46}$	0.20 – 0.77	19 – 64	47 – 79	1.8 – 1.9	0.0 – 2.0	-
	$\mathsf{T}^5_{26,34}$	0.0 – 1.0	32 – 38	32 – 35	0.64 – 1.4	0.44 – 1.6	-
	$\mathsf{T}^4_{26,35}$	0.10 – 0.65	13 – 19	36 – 39	≈ 1.5	0.47 – 0.81	-
	$\mathsf{T}^2_{35,46}$	0.23 – 0.80	19 – 66	47 – 80	0.094 – 0.18	0.0 – 2.0	✓

Table 7. Neutrino mass textures in class $2_2 1_1 0_1$ compatible with data at 3σ CL for IO spectrum.

Spectrum	Texture	δ/π	m [meV]	$m_{\beta\beta}$ [meV]	α_{21}/π	α_{31}/π	1σ CL
NO	T^3_{125}	0.19 – 0.63	20 – 24	16 – 18	≈ 1.6	1.5 – 1.9	-
	T^6_{134}	0.0 – 0.90	53 – 60	34 – 39	0.54 – 1.5	0.45 – 1.6	-
	T^2_{135}	0.32 – 0.85	20 – 24	15 – 18	0.38 – 0.46	0.096 – 0.47	✓
	T^2_{136}	0.38 – 0.46	11 – 13	9.7 – 11	≈ 1.5	0.66 – 0.76	-
	T^3_{145}	0.16 – 0.25	29 – 39	29 – 40	0.052 – 0.17	0.55 – 0.62	✓
		0.80 – 0.93	29 – 39	29 – 40	0.060 – 0.18	1.5 – 1.7	
	T^2_{145}	0.087 – 0.21	30 – 41	30 – 41	≈ 1.9	0.39 – 0.53	✓
		0.72 – 0.83	30 – 40	30 – 41	≈ 1.9	1.3 – 1.5	
	T^3_{146}	0.096 – 0.94	16 – 69	17 – 69	0.045 – 0.23	0.33 – 1.7	✓
	T^2_{146}	0.062 – 0.91	16 – 69	16 – 69	1.8 – 2.0	0.25 – 1.7	✓
	T^3_{156}	0.16 – 0.24	28 – 39	29 – 39	0.081 – 0.11	0.52 – 0.63	✓
		0.81 – 0.93	29 – 38	29 – 39	0.10 – 0.12	1.5 – 1.6	
	T^2_{156}	0.060 – 0.18	29 – 38	28 – 39	1.8 – 1.9	0.31 – 0.50	✓
		0.76 – 0.85	28 – 38	28 – 39	1.8 – 1.9	≈ 1.4	
	T^6_{234}	0.0 – 1.0	54 – 71	48 – 70	0.12 – 2.0	0.86 – 1.3	✓
	T^4_{236}	0.0 – 1.0	54 – 72	48 – 70	0.036 – 1.9	0.74 – 1.1	✓
IO	T^6_{123}	0.0 – 1.0	9.4 – 57	27 – 43	0.62 – 1.4	0.34 – 1.8	-
	T^5_{123}	0.0 – 0.40	31 – 36	33 – 36	0.64 – 1.4	0.43 – 1.6	✓
		0.51 – 1.0	32 – 36	33 – 36	0.64 – 1.4	0.43 – 1.6	
	T^4_{123}	0.0 – 1.0	9.5 – 56	27 – 43	0.62 – 1.4	0.24 – 1.6	✓
	T^6_{125}	0.0 – 1.0	25 – 37	28 – 38	0.61 – 1.4	0.37 – 1.8	✓
	T^4_{125}	0.0 – 1.0	25 – 39	27 – 38	0.60 – 1.4	0.25 – 1.8	✓
	T^5_{126}	0.17 – 0.41	29 – 37	27 – 37	0.62 – 0.85	0.45 – 0.72	✓
		0.72 – 0.93	29 – 37	27 – 37	1.1 – 1.4	1.2 – 1.6	
	T^5_{134}	0.061 – 0.23	30 – 39	29 – 39	0.61 – 0.80	0.38 – 0.74	✓
		0.62 – 0.84	30 – 39	29 – 39	1.2 – 1.4	1.3 – 1.6	
	T^6_{135}	0.0 – 1.0	30 – 39	31 – 38	0.60 – 1.4	0.40 – 1.7	✓
	T^4_{135}	0.0 – 1.0	26 – 37	28 – 38	0.60 – 1.4	0.23 – 1.6	✓
	T^6_{145}	0.36 – 0.96	13 – 20	12 – 17	0.86 – 1.1	0.0011 – 2.0	-
	T^4_{156}	0.055 – 0.66	13 – 20	12 – 17	0.86 – 1.1	0.0 – 2.0	-
	T^6_{234}	0.0 – 0.32	30 – 66	48 – 78	0.21 – 1.9	0.81 – 1.3	-
		0.60 – 1.0	22 – 66	43 – 78	0.22 – 1.9	0.85 – 1.3	
	T^5_{234}	0.0 – 0.45	29 – 38	29 – 39	0.63 – 1.4	0.42 – 1.6	✓
		0.58 – 1.0	29 – 38	29 – 39	0.68 – 1.4	0.46 – 1.6	
	T^6_{235}	0.0 – 1.0	15 – 49	33 – 38	0.51 – 1.4	0.23 – 1.8	-
	T^4_{235}	0.0 – 1.0	14 – 49	33 – 38	0.59 – 1.5	0.24 – 1.8	✓
	T^5_{236}	0.0 – 0.97	25 – 37	27 – 37	0.62 – 1.4	0.42 – 1.5	✓
	T^4_{236}	0.0 – 1.0	15 – 66	38 – 78	0.12 – 1.8	0.54 – 1.2	-
	T^5_{246}	0.13 – 0.31	27 – 38	27 – 37	0.62 – 0.84	0.45 – 0.71	✓
		0.63 – 0.89	27 – 38	27 – 37	1.2 – 1.4	1.2 – 1.6	
	T^4_{256}	0.17 – 0.59	13 – 16	35 – 38	1.4 – 1.5	0.46 – 0.79	-
	T^5_{346}	0.098 – 0.31	29 – 40	29 – 39	0.61 – 0.80	0.39 – 0.73	✓
		0.72 – 0.87	29 – 39	28 – 39	1.2 – 1.4	1.3 – 1.6	
	T^4_{356}	0.21 – 0.58	13 – 16	36 – 39	≈ 1.5	0.50 – 0.79	-
	T^3_{456}	0.48 – 0.51	0.96 – 1.4	45 – 49	≈ 1.9	1.9 – 2.0	-
	T^2_{456}	0.49 – 0.52	0.96 – 1.4	45 – 49	0.096 – 0.12	0.024 – 0.065	-

Table 8. Neutrino mass textures in class $3_1 1_2 0_1$ compatible with data at 3σ CL.

Spectrum	Texture	δ/π	m [meV]	$m_{\beta\beta}$ [meV]	α_{21}/π	α_{31}/π	1σ CL
NO	$\mathsf{T}_{124,36}$	0.0 – 1.0	31 – 35	17 – 22	0.58 – 1.4	0.25 – 1.7	✓
	$\mathsf{T}_{125,46}$	0.0 – 0.98	21 – 42	16 – 21	0.63 – 1.6	0.36 – 1.8	✓
	$\mathsf{T}_{126,34}$	0.0 – 1.0	29 – 35	16 – 24	0.55 – 1.4	0.12 – 1.9	✓
	$\mathsf{T}_{126,45}$	0.0 – 1.0	20 – 31	10 – 13	0.60 – 1.4	0.0 – 2.0	✓
	$\mathsf{T}_{134,26}$	0.0 – 1.0	29 – 35	16 – 24	0.56 – 1.4	0.14 – 1.9	✓
	$\mathsf{T}_{134,56}$	0.29 – 1.0	26 – 31	11 – 13	0.73 – 1.3	0.0 – 2.0	-
	$\mathsf{T}_{135,46}$	0.0 – 1.0	21 – 44	16 – 22	0.38 – 1.4	0.20 – 1.6	✓
	$\mathsf{T}_{136,24}$	0.0 – 1.0	31 – 35	17 – 22	0.59 – 1.4	0.27 – 1.7	✓
	$\mathsf{T}_{136,45}$	0.25 – 0.58	11 – 14	9.5 – 12	≈ 1.5	0.57 – 0.80	-
	$\mathsf{T}_{145,23}$	0.29 – 0.32	29 – 39	29 – 40	1.9 – 2.0	0.41 – 0.56	✓
		0.61 – 0.63	29 – 39	30 – 40	1.9 – 2.0	1.4 – 1.5	
	$\mathsf{T}_{156,23}$	0.37 – 0.40	29 – 38	29 – 39	0.045 – 0.11	0.52 – 0.58	✓
		0.68 – 0.71	28 – 38	28 – 39	0.032 – 0.093	1.5 – 1.6	
	$\mathsf{T}_{234,16}$	0.0 – 1.0	22 – 51	18 – 30	0.072 – 1.9	0.0 – 2.0	✓
	$\mathsf{T}_{236,14}$	0.0 – 1.0	22 – 48	19 – 30	0.14 – 2.0	0.026 – 1.4	✓
	$\mathsf{T}_{246,13}$	0.0 – 1.0	25 – 40	12 – 26	0.56 – 1.4	0.22 – 1.8	✓
	$\mathsf{T}_{256,14}$	0.38 – 1.0	44 – 51	13 – 15	0.87 – 1.1	0.0 – 2.0	-
	$\mathsf{T}_{345,16}$	0.0 – 0.78	44 – 54	13 – 15	0.86 – 1.1	0.0 – 2.0	-
	$\mathsf{T}_{346,12}$	0.0 – 1.0	25 – 40	12 – 26	0.55 – 1.4	0.14 – 1.8	✓
	$\mathsf{T}_{356,12}$	0.60 – 1.0	18 – 21	3.8 – 5.2	0.86 – 1.1	0.64 – 1.1	-
IO	$\mathsf{T}_{123,45}$	0.0 – 1.0	7.0 – 11	27 – 29	0.63 – 1.4	0.0 – 2.0	✓
	$\mathsf{T}_{123,56}$	0.0 – 1.0	7.4 – 11	27 – 30	0.63 – 1.4	0.0013 – 2.0	✓
	$\mathsf{T}_{125,46}$	0.13 – 0.43	33 – 50	35 – 39	1.2 – 1.4	0.10 – 0.80	✓
		0.59 – 0.86	24 – 29	27 – 30	0.69 – 0.82	1.4 – 1.8	
	$\mathsf{T}_{126,45}$	0.0 – 0.69	20 – 30	30 – 35	0.67 – 1.4	0.93 – 2.0	-
	$\mathsf{T}_{134,56}$	0.30 – 0.43	53 – 60	47 – 52	0.53 – 0.59	0.0 – 2.0	-
		0.82 – 0.95	53 – 61	47 – 52	0.54 – 0.58	0.83 – 0.90	
	$\mathsf{T}_{135,46}$	0.53 – 0.83	33 – 49	35 – 39	0.61 – 0.75	1.2 – 1.9	✓
	$\mathsf{T}_{234,56}$	0.0 – 0.32	8.1 – 21	32 – 49	0.44 – 1.7	0.0068 – 2.0	✓
		0.66 – 1.0	8.0 – 20	32 – 49	0.54 – 1.7	0.69 – 1.3	
	$\mathsf{T}_{236,45}$	0.0 – 1.0	7.1 – 18	28 – 47	0.30 – 1.6	0.0 – 2.0	✓
	$\mathsf{T}_{245,36}$	0.0 – 0.095	9.2 – 16	37 – 42	0.44 – 1.6	0.19 – 1.9	✓
		0.74 – 0.87	9.5 – 16	37 – 42	1.5 – 1.6	1.1 – 1.2	
	$\mathsf{T}_{246,13}$	0.12 – 0.48	3.7 – 45	30 – 37	0.57 – 0.76	0.40 – 0.65	✓
		0.75 – 1.0	5.0 – 47	30 – 37	0.57 – 1.4	0.25 – 1.6	
	$\mathsf{T}_{246,35}$	0.0 – 1.0	8.3 – 18	38 – 41	0.42 – 1.6	0.0 – 2.0	✓
	$\mathsf{T}_{256,34}$	0.0 – 1.0	2.9 – 6.4	36 – 42	0.41 – 1.6	0.0 – 2.0	-
	$\mathsf{T}_{345,26}$	0.0 – 1.0	2.9 – 6.4	36 – 42	0.38 – 1.6	0.0 – 2.0	-
	$\mathsf{T}_{346,12}$	0.0 – 0.25	12 – 50	30 – 38	0.60 – 0.77	0.36 – 0.65	✓
		0.68 – 0.88	11 – 51	30 – 38	1.2 – 1.4	1.4 – 1.6	
	$\mathsf{T}_{346,25}$	0.0 – 1.0	8.3 – 21	38 – 42	0.42 – 1.6	0.0 – 2.0	-
	$\mathsf{T}_{356,24}$	0.14 – 0.31	8.5 – 14	37 – 42	0.39 – 0.49	0.80 – 0.98	✓
		0.85 – 1.0	8.6 – 14	38 – 42	0.39 – 1.6	0.13 – 1.8	
	$\mathsf{T}_{456,12}$	0.0 – 0.51	1.5 – 2.7	23 – 31	0.60 – 1.4	0.0 – 2.0	✓
		0.62 – 1.0	1.5 – 2.7	23 – 31	0.69 – 1.4	0.11 – 1.2	
	$\mathsf{T}_{456,13}$	0.026 – 1.0	1.4 – 2.5	24 – 33	0.56 – 1.4	0.0 – 2.0	✓

Table 9. Neutrino mass textures in class $3_1 2_1 1_1$ compatible with data at 3σ CL.

Spectrum	Texture	δ/π	m [meV]	$m_{\beta\beta}$ [meV]	α_{21}/π	α_{31}/π	1σ CL
NO	T_{1234}	0.21 – 1.0	20 – 51	13 – 30	0.54 – 1.4	0.58 – 1.7	✓
	T_{1235}	0.0 – 0.32	30 – 34	18 – 20	0.64 – 1.4	0.40 – 1.6	✓
		0.63 – 0.96	31 – 34	18 – 20	1.3 – 1.4	1.4 – 1.6	
	T_{1236}	0.0 – 0.20	20 – 44	12 – 26	0.56 – 1.5	0.57 – 1.4	✓
		0.57 – 0.79	17 – 43	11 – 26	1.3 – 1.5	0.36 – 0.53	
	T_{1246}	0.0 – 1.0	26 – 41	18 – 22	0.58 – 1.4	0.26 – 1.7	✓
	T_{1346}	0.0 – 1.0	26 – 41	18 – 22	0.60 – 1.4	0.25 – 1.7	✓
IO	T_{2345}	0.0 – 0.45	11 – 13	36 – 44	0.37 – 1.6	0.62 – 1.4	-
		0.73 – 1.0	10 – 13	36 – 44	0.42 – 1.6	0.063 – 1.8	
	T_{2356}	0.0 – 0.99	11 – 13	36 – 43	0.38 – 1.6	0.21 – 1.9	✓
	T_{2456}	0.0 – 1.0	1.1 – 1.9	32 – 44	0.39 – 1.7	0.0 – 2.0	✓
	T_{3456}	0.0 – 1.0	1.1 – 1.8	33 – 44	0.32 – 1.6	0.0 – 2.0	✓

Table 10. Neutrino mass textures in class $4_1 1_2$ compatible with data at 3σ CL.

Spectrum	Texture	δ/π	m [meV]	$m_{\beta\beta}$ [meV]	α_{21}/π	α_{31}/π	1σ CL
NO	$\mathsf{T}_{12,35,46}$	0.0 – 1.0	22 – 47	8.4 – 31	0.61 – 1.5	0.42 – 1.7	✓
	$\mathsf{T}_{13,25,46}$	0.0 – 0.99	22 – 44	8.5 – 29	0.55 – 1.4	0.38 – 1.6	✓
	$\mathsf{T}_{14,23,56}$	0.33 – 0.51	19 – 45	20 – 46	0.059 – 0.080	0.52 – 0.66	✓
		0.68 – 0.72	18 – 44	20 – 45	0.035 – 0.062	1.4 – 1.6	
	$\mathsf{T}_{16,23,45}$	0.16 – 0.65	12 – 39	13 – 40	1.9 – 2.0	0.45 – 1.5	✓
IO	$\mathsf{T}_{14,23,56}$	0.32 – 1.0	6.7 – 8.3	12 – 24	0.73 – 1.2	0.27 – 1.1	-
	$\mathsf{T}_{16,23,45}$	0.0 – 0.68	6.6 – 8.3	12 – 28	0.77 – 1.3	0.87 – 1.7	✓

Table 11. Neutrino mass textures in class 2_3 compatible with data at 3σ CL.

Spectrum	Texture	δ/π	m [meV]	$m_{\beta\beta}$ [meV]	α_{21}/π	α_{31}/π	1σ CL
NO	T_{123}	0.0 – 1.0	1.5 – 51	4.8 – 30	0.0 – 2.0	0.0 – 2.0	✓
	T_{124}	0.0 – 1.0	13 – 69	11 – 36	0.48 – 1.4	0.25 – 1.7	✓
	T_{125}	0.0 – 0.99	20 – 63	16 – 39	0.52 – 1.6	0.0014 – 2.0	✓
	T_{126}	0.0 – 1.0	13 – 62	9.6 – 40	0.36 – 1.6	0.0 – 2.0	✓
	T_{134}	0.0 – 1.0	17 – 67	11 – 43	0.47 – 1.5	0.0 – 2.0	✓
	T_{135}	0.0 – 1.0	20 – 64	15 – 40	0.38 – 1.5	0.0 – 2.0	✓
	T_{136}	0.0 – 1.0	11 – 67	9.7 – 35	0.57 – 1.5	0.26 – 1.7	✓
	T_{145}	0.0 – 1.0	28 – 63	30 – 52	0.0 – 2.0	0.098 – 1.9	✓
	T_{146}	0.0 – 1.0	15 – 70	16 – 70	0.0 – 2.0	0.12 – 1.9	✓
	T_{156}	0.0 – 1.0	27 – 63	28 – 47	0.0 – 2.0	0.16 – 2.0	✓
	T_{234}	0.0 – 1.0	18 – 71	5.9 – 72	0.0 – 2.0	0.0011 – 2.0	✓
	T_{235}	0.0 – 1.0	31 – 71	9.5 – 71	0.0 – 2.0	0.0 – 2.0	✓
	T_{236}	0.0 – 1.0	14 – 71	4.6 – 71	0.0 – 2.0	0.0029 – 2.0	✓
	T_{245}	0.0 – 1.0	20 – 66	3.6 – 46	0.59 – 1.5	0.0017 – 2.0	✓
	T_{246}	0.0 – 1.0	26 – 71	7.1 – 71	0.0 – 2.0	0.0 – 2.0	✓
	T_{256}	0.0 – 1.0	37 – 71	7.4 – 33	0.70 – 1.3	0.0 – 2.0	✓
	T_{345}	0.0 – 1.0	39 – 71	8.5 – 36	0.71 – 1.3	0.0 – 2.0	✓
	T_{346}	0.0 – 1.0	26 – 71	7.1 – 71	0.0 – 2.0	0.0 – 2.0	✓
	T_{356}	0.012 – 1.0	18 – 52	3.5 – 37	0.49 – 1.4	0.0017 – 2.0	✓
IO	T_{123}	0.0 – 1.0	0.21 – 64	27 – 47	0.62 – 1.4	0.0 – 2.0	✓
	T_{125}	0.0 – 1.0	25 – 60	27 – 47	0.59 – 1.4	0.030 – 2.0	✓
	T_{126}	0.0 – 1.0	9.7 – 61	27 – 48	0.61 – 1.5	0.028 – 2.0	✓
	T_{134}	0.0 – 1.0	14 – 60	29 – 47	0.53 – 1.4	0.025 – 1.9	✓
	T_{135}	0.0 – 1.0	26 – 61	29 – 48	0.57 – 1.4	0.11 – 2.0	✓
	T_{145}	0.0 – 1.0	12 – 60	11 – 40	0.69 – 1.2	0.0 – 2.0	✓
	T_{146}	0.0 – 0.99	5.1 – 65	12 – 67	0.41 – 1.6	0.020 – 2.0	✓
	T_{156}	0.0 – 1.0	12 – 62	11 – 38	0.76 – 1.3	0.0 – 2.0	✓
	T_{234}	0.0 – 1.0	0.97 – 66	30 – 82	0.0 – 2.0	0.0088 – 2.0	✓
	T_{235}	0.0 – 1.0	3.5 – 65	33 – 80	0.0 – 2.0	0.0 – 2.0	✓
	T_{236}	0.0 – 1.0	0.66 – 66	27 – 81	0.0 – 2.0	0.0028 – 2.0	✓
	T_{245}	0.0 – 1.0	0.17 – 64	28 – 64	0.38 – 1.7	0.0 – 2.0	✓
	T_{246}	0.0 – 1.0	0.79 – 65	27 – 81	0.0015 – 2.0	0.0076 – 2.0	✓
	T_{256}	0.0 – 1.0	0.22 – 60	32 – 55	0.38 – 1.7	0.0 – 2.0	✓
	T_{345}	0.0 – 1.0	0.11 – 65	34 – 54	0.30 – 1.6	0.0017 – 2.0	✓
	T_{346}	0.0 – 1.0	0.14 – 66	29 – 80	0.0 – 2.0	0.0 – 2.0	✓
	T_{356}	0.0 – 1.0	0.34 – 62	32 – 60	0.28 – 1.6	0.0040 – 2.0	✓
	T_{456}	0.0 – 1.0	0.94 – 5.2	12 – 50	0.0 – 2.0	0.0 – 2.0	✓

Table 12. Neutrino mass textures in class $3_1 1_3$ compatible with data at 3σ CL.

B Extra correlations among the elements of $\mathbf{m}_\nu$ in class $2_1 1_2 0_2$

In this appendix, we analyse the textures belonging to class $2_1 1_2 0_2$ (cf. table 5) with the aim of looking for extra correlations among the matrix elements of $\mathbf{m}_\nu$ in the spirit of [27]. From our search, the textures

$$\mathsf{T}_{45}^{1,2} = \begin{pmatrix} 0 & 0 & a \\ 0 & b & b \\ a & b & c \end{pmatrix} , \quad \mathsf{T}_{45}^{1,3} = \begin{pmatrix} 0 & a & 0 \\ a & b & b \\ 0 & b & c \end{pmatrix} , \tag{B.1}$$

$$\mathsf{T}_{46}^{1,2} = \begin{pmatrix} 0 & 0 & a \\ 0 & b & c \\ a & c & b \end{pmatrix} , \quad \mathsf{T}_{46}^{1,3} = \begin{pmatrix} 0 & a & 0 \\ a & b & c \\ 0 & c & b \end{pmatrix} , \tag{B.2}$$

$$\mathsf{T}_{56}^{1,2} = \begin{pmatrix} 0 & 0 & a \\ 0 & c & b \\ a & b & b \end{pmatrix} , \quad \mathsf{T}_{56}^{1,3} = \begin{pmatrix} 0 & a & 0 \\ a & c & b \\ 0 & b & b \end{pmatrix} , \tag{B.3}$$

led to interesting correlations for NO neutrino mass spectrum. In figures 3(a)–3(f), we plot the ratio $|c|/|a|$ versus the ratio $|b|/|a|$ for each of these textures. The plots show the allowed regions at the 1σ CL (red points) and 3σ CL (blue points). As can be seen from the figures, these ratios always lie approximately between 3/2 and 3. Imposing an extra correlation among the input parameters a, b and c, we have found several patterns that are compatible with data. These textures are summarised in table 13. In addition to the two textures found in [27], which correspond to the matrices (B.2) with $c = 2a$, there are eight new textures that are consistent with observations at 3σ CL, after reducing the number of physical parameters from four to three. Remarkably, the textures

$$\begin{pmatrix} 0 & 0 & 2a \\ 0 & b & b \\ 2a & b & 5a \end{pmatrix} , \quad \begin{pmatrix} 0 & 0 & 2a \\ 0 & 5a & b \\ 2a & b & 5a \end{pmatrix} , \quad \begin{pmatrix} 0 & 2a & 0 \\ 2a & 5a & b \\ 0 & b & 5a \end{pmatrix} , \quad \begin{pmatrix} 0 & 2a & 0 \\ 2a & 5a & b \\ 0 & b & b \end{pmatrix} , \tag{B.4}$$

with a real and b complex (or vice-versa), are compatible with observations even at 1σ CL.

Texture	Correlation	$a, b, c \in \mathbb{C}$	$a, b, c \in \mathbb{R}$
$\mathsf{T}_{45}^{1,2}$ $(A_{1,45})$	$c = 2a$ or $c = 3a$	✓	–
$\mathsf{T}_{45}^{1,3}$ $(A_{2,45})$	$b = 2a$ or $c = 2a$	✓	–
$\mathsf{T}_{46}^{1,2}$ $(A_{1,46})$	$c = 2a$	✓	✓
$\mathsf{T}_{46}^{1,3}$ $(A_{2,46})$	$c = 2a$	✓	✓
$\mathsf{T}_{56}^{1,2}$ $(A_{1,56})$	$b = 2a$ or $c = 2a$	✓	–
$\mathsf{T}_{56}^{1,3}$ $(A_{2,56})$	$c = 2a$ or $c = 3a$	✓	–

Table 13. Particular cases of extra correlations that can be imposed on the textures of table 5. In all cases, the resulting $\mathbf{m}_\nu$ contains only three physical parameters. The checkmark indicates whether the texture with the given correlation is compatible with neutrino oscillation data at 3σ CL.

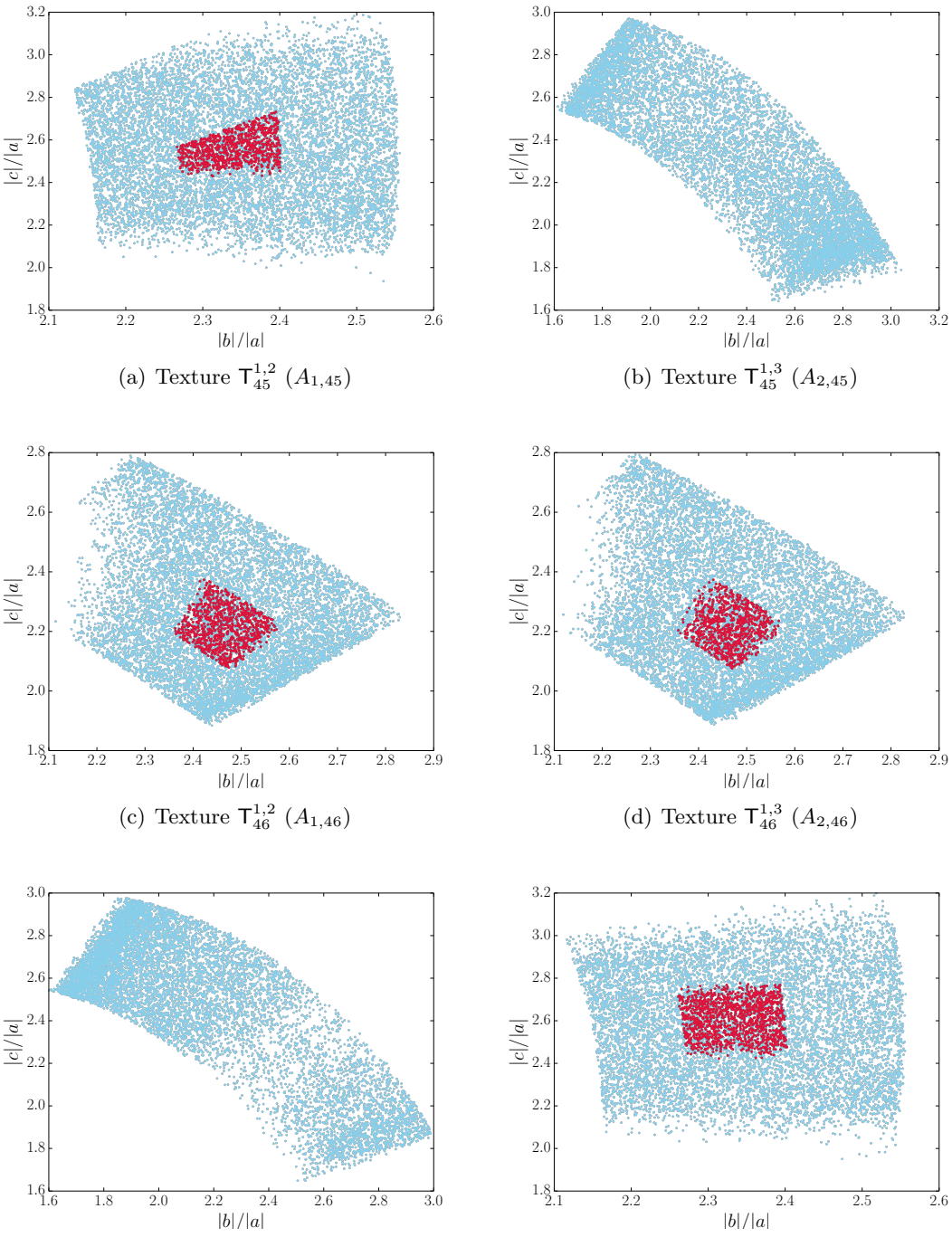

(a) Texture $\mathsf{T}_{45}^{1,2}$ $(A_{1,45})$ (b) Texture $\mathsf{T}_{45}^{1,3}$ $(A_{2,45})$

(c) Texture $\mathsf{T}_{46}^{1,2}$ $(A_{1,46})$ (d) Texture $\mathsf{T}_{46}^{1,3}$ $(A_{2,46})$

(e) Texture $\mathsf{T}_{56}^{1,2}$ $(A_{1,56})$ (f) Texture $\mathsf{T}_{56}^{1,3}$ $(A_{2,56})$

Figure 3. Correlations among the moduli of the physical parameters of the viable textures within class $2_1 1_2 0_2$ for NO spectrum (see table 5). The red and blue points in the scatter plots correspond to solutions compatible with neutrino data at the 1σ and 3σ CL, respectively.

References

[1] G. C. Branco, D. Emmanuel-Costa and R. González Felipe, *Texture zeros and weak basis transformations*, *Phys. Lett. B* **477** (2000) 147–155, [hep-ph/9911418].

[2] G. C. Branco, D. Emmanuel-Costa, R. González Felipe and H. Serôdio, *Weak Basis Transformations and Texture Zeros in the Leptonic Sector*, *Phys. Lett. B* **670** (2009) 340–349, [0711.1613].

[3] W. Grimus, A. S. Joshipura, L. Lavoura and M. Tanimoto, *Symmetry realization of texture zeros*, *Eur. Phys. J. C* **36** (2004) 227–232, [hep-ph/0405016].

[4] R. González Felipe and H. Serôdio, *Abelian realization of phenomenological two-zero neutrino textures*, *Nucl. Phys. B* **886** (2014) 75–92, [1405.4263].

[5] P. H. Frampton, S. L. Glashow and D. Marfatia, *Zeroes of the neutrino mass matrix*, *Phys. Lett. B* **536** (2002) 79–82, [hep-ph/0201008].

[6] H. Fritzsch, Z.-z. Xing and S. Zhou, *Two-zero Textures of the Majorana Neutrino Mass Matrix and Current Experimental Tests*, *JHEP* **09** (2011) 083, [1108.4534].

[7] D. Meloni and G. Blankenburg, *Fine-tuning and naturalness issues in the two-zero neutrino mass textures*, *Nucl. Phys. B* **867** (2013) 749–762, [1204.2706].

[8] D. Meloni, A. Meroni and E. Peinado, *Two-zero Majorana textures in the light of the Planck results*, *Phys. Rev. D* **89** (2014) 053009, [1401.3207].

[9] L. M. Cebola, D. Emmanuel-Costa and R. G. Felipe, *Confronting predictive texture zeros in lepton mass matrices with current data*, *Phys. Rev. D* **92** (2015) 025005, [1504.06594].

[10] S. Kaneko, H. Sawanaka and M. Tanimoto, *Hybrid textures of neutrinos*, *JHEP* **08** (2005) 073, [hep-ph/0504074].

[11] J.-Y. Liu and S. Zhou, *Hybrid Textures of Majorana Neutrino Mass Matrix and Current Experimental Tests*, *Phys. Rev. D* **87** (2013) 093010, [1304.2334].

[12] F. Capozzi, G. L. Fogli, E. Lisi, A. Marrone, D. Montanino and A. Palazzo, *Status of three-neutrino oscillation parameters, circa 2013*, *Phys. Rev. D* **89** (2014) 093018, [1312.2878].

[13] D. V. Forero, M. Tórtola and J. W. F. Valle, *Neutrino oscillations refitted*, *Phys. Rev. D* **90** (2014) 093006, [1405.7540].

[14] M. C. Gonzalez-Garcia, M. Maltoni and T. Schwetz, *Global Analyses of Neutrino Oscillation Experiments*, 1512.06856.

[15] Planck collaboration, P. A. R. Ade et al., *Planck 2015 results. XIII. Cosmological parameters*, 1502.01589.

[16] G. C. Branco, R. G. Felipe and F. R. Joaquim, *Leptonic CP Violation*, *Rev. Mod. Phys.* **84** (2012) 515–565, [1111.5332].

[17] LBNE collaboration, C. Adams et al., *The Long-Baseline Neutrino Experiment: Exploring Fundamental Symmetries of the Universe*, 1307.7335.

[18] B. Pontecorvo, *Inverse beta processes and nonconservation of lepton charge*, *Sov. Phys. JETP* **7** (1958) 172–173.

[19] Z. Maki, M. Nakagawa and S. Sakata, *Remarks on the unified model of elementary particles*, *Prog. Theor. Phys.* **28** (1962) 870–880.

[20] B. Pontecorvo, *Neutrino Experiments and the Problem of Conservation of Leptonic Charge*, *Sov. Phys. JETP* **26** (1968) 984–988.

[21] Particle Data Group collaboration, K. A. Olive et al., *Review of Particle Physics*, *Chin. Phys. C* **38** (2014) 090001.

[22] F. James and M. Roos, *Minuit: A System for Function Minimization and Analysis of the Parameter Errors and Correlations*, *Comput. Phys. Commun.* **10** (1975) 343–367.

[23] T2K collaboration, K. Abe et al., *Observation of Electron Neutrino Appearance in a Muon Neutrino Beam*, *Phys. Rev. Lett.* **112** (2014) 061802, [1311.4750].

[24] CUORE collaboration, K. Alfonso et al., *Search for Neutrinoless Double-Beta Decay of ^{130}Te with CUORE-0*, *Phys. Rev. Lett.* **115** (2015) 102502, [1504.02454].

[25] NEMO-3, SuperNEMO collaboration, A. Remoto, *Latest results from NEMO-3 and status of SuperNEMO*, *Nucl. Part. Phys. Proc.* **265-266** (2015) 67–69.

[26] M. Frigerio and A. Villanova del Moral, *Minimal lepton flavour structures lead to non-maximal 2-3 mixing*, *JHEP* **07** (2013) 146, [1303.5284].

[27] W. Grimus and P. O. Ludl, *Two-parameter neutrino mass matrices with two texture zeros*, *J. Phys. G* **40** (2013) 055003, [1208.4515].

[28] L. M. Cebola, D. Emmanuel-Costa and R. González Felipe, *Anomaly-free U(1) gauge symmetries in neutrino seesaw flavor models*, *Phys. Rev. D* **88** (2013) 116008, [1309.1709].